Available online at www.sciencedirect.com
ScienceDirect
Ceramics International 38 (2012) 787–793
CERAMICS INTERNATIONAL
www.elsevier.com/locate/ceramint

Pore size control of Al_2O_3 ceramics using two-step sintering

Toshihiro Isobe *, Asami Ooyama, Mai Shimizu, Akira Nakajima

Graduate School of Science and Engineering, Tokyo Institute of Technology, 2-12-1 Ookayama, Meguro-ku, Tokyo 152-8550, Japan

Received 14 May 2011; received in revised form 15 July 2011; accepted 1 August 2011
Available online 10th August 2011

Abstract

Porous Al_2O_3 ceramics were prepared using a two-step sintering method. Green bodies were prepared using the slip cast method. The average pore size and porosity of the obtained samples were, respectively, 73 nm and 42%. The porosities and the average pore size of the samples prepared using a one-step sintering method decreased concomitantly with increasing sintering temperature. The porosity was mostly constant at temperatures higher than 1300 °C. The T_1 and T_2 temperatures were set, respectively as 1150 °C and 1000 °C for two-step sintering tests. Under these conditions, the pore size was controllable by sintering time without porosity change. The average pore size of the obtained samples was 61–76 nm without porosity change.

Keywords: Ceramics; Nanostructures; Structural materials; Microstructure

1. Introduction

Porous ceramics are widely used in industrial, catalyst, and environmental fields. Various methods for their preparation have been studied [1]. The replica method includes the impregnation of a porous structure with ceramic slurries or a precursor solution to prepare porous ceramics [2–8]. This method is available to prepare porous ceramics having a simple, complicated, or unique structure. Using a polymeric sponge as the template, the obtained porous ceramics have 40–95% porosity and 0.2–3 mm pore or hole size [2–5], which is probably suitable for high-throughput filtration. Natural woods can be processed using this method [6–8]. In the sacrificial template method, organic additives are mixed with ceramic powders and are burned out during sintering of the molded green bodies. Synthetic organic powders [5,9–13] and fibers [12–14] have been used as pore formers. The foaming method incorporates air into ceramic slurries or liquid precursor and maintains the structure that is constructed by the air bubbles [15–19]. The pore size and porosity depend on the rheological properties of the precursors. Porous ceramics prepared using these methods show excellent microstructures and properties. Consequently, porous ceramics are used in many end products.

Partial sintering, an extremely straightforward and simple technique, is another method used to prepare porous ceramics [20–24]. The powder compacts are heated at less than optimum sintering temperature for preparation of the dense body. The pore size and porosity of the porous ceramics depend on the particle size and porosity of the green body. They are also controllable using a heating program. The ceramics sintered at high temperatures generally have low porosity and small pores because of matrix densification. Therefore, the sintering program is an important factor to be considered in preparing porous ceramics. This method also has an important shortcoming: pore size control of 10 nm order is difficult.

Two-step sintering is a remarkable sintering program [25,26]. This technique uses the difference of reaction velocities between the diffusion of atoms and the grain boundary migration. The resultant ceramics have high relative density and low grain growth. Diffusion of the atoms and grain boundary migration are thought to be independent parameters during sintering by this program. Therefore, this method is useful to control the pore size or porosity precisely. In this study, porous Al_2O_3 ceramics were prepared using two-step sintering. The relations between the heating program and the porosity and pore size were investigated.

* Corresponding author. Tel.: +81 3 5734 2525; fax: +81 3 5734 3355.
E-mail address: isobe.t.ad@m.titech.ac.jp (T. Isobe).

0272-8842/$36.00.
doi:10.1016/j.ceramint.2011.08.005

2. Experimental procedure

2.1. Preparation of green bodies

First, 30% (vol) high purity α-Al_2O_3 (TM-DAR; Taimei Chemicals Co. Ltd., Nagano, Japan) was mixed with 70% (vol) distilled water and 0.62% (mass) poly(ammonium acrylate) (PAA) (Ceruna D-305; Chukyo Yushi Co. Ltd., Aichi, Japan) as a dispersant. Mixing was done using a planetary-type mixer [27] without stainless steel mesh for 1 min, rotated at 800 rpm, and revolved at 2000 rpm for 1 min. Then, the mixtures were treated for 10 min using a mixer with the mesh to disperse the α-Al_2O_3 particles in the slurry. After mesh treatment, the suspensions were re-mixed without mesh for 1 min to remove bubbles. The respective rotation and revolution rates were 60 and 2000 rpm. The resulting slurries were slip-casted into a 16 mmϕ gypsum mold for 5 min. They were dried at room temperature for 24 h and were heated at 800 °C for 2 h to burn out the dispersant. The microstructures of the present samples were observed using a field emission scanning electron microscope (FE-SEM, S4500; Hitachi High-Technologies Corp., Tokyo, Japan).

2.2. Sintering of ceramic bodies

In the case of single-step sintering, the green bodies were sintered at 1000–1400 °C for 2 h. The heating and cooling rates were 100 °C/h. The sintering program of the two-step sintering is presented in Fig. 1. Temperatures of the first sintering step (T_1) and the second sintering step (T_2) are presented in Table 1. Several combinations of temperatures of T_1, T_2, and keeping time of T_2 (t) were used for this study. The heating rate of up to the T_1 for all programs was 100 °C/h. The respective cooling rates from T_1 to T_2 and from T_2 to room temperature were 15 °C/min and 100 °C/h. For program A, the T_1 was 1000–1300 °C and the T_2 was set the 150 °C lower than T_1. The t was

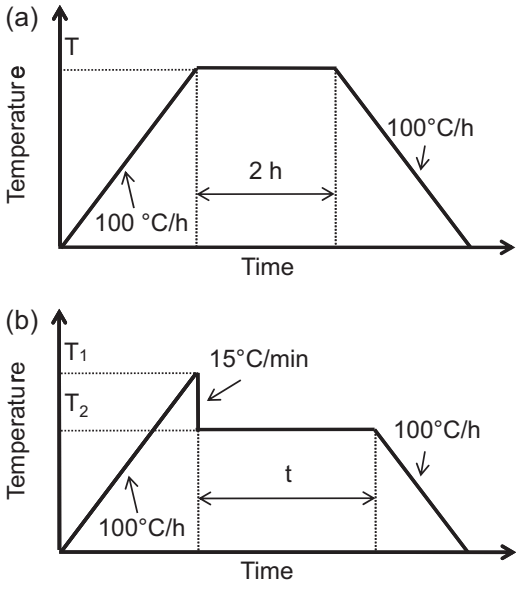

Fig. 1. Heating programs of (a) single and (b) two-step sintering methods.

Table 1
Sintering program for a two-step sintering study.

	T_1 (°C)	T_2 (°C)	t [h]
A	1000–1300	T_1 minus 150	12
B	1000–1250	1000	12
C	1150	1000	2–12

12 h. Regarding program B, the effect of the T_1 for the porous structure of the samples was evaluated. The values of T_2 and t were, respectively, 1000 °C and 12 h. The t dependence was evaluated using the program *C*. The values of T_1 and the t were, respectively, 1000 °C and 2–12 h.

After sintering, the surfaces of all samples were polished using commercial #400 and #1500 emery. The samples were washed ultrasonically for 10 min in de-ionized purified water. Then the densities and porosities of the samples were measured using Archimedes' technique with water. The linear shrinkage was calculated using Eq. (1).

$$\frac{D_b - D_a}{D_b} \times 100 \quad (1)$$

In Eq. (1), D_b and D_a, respectively denote the diameters of the sample before and after sintering. The pore size distribution of the samples was measured using mercury intrusion porosimetry (Pascal 140 and Pascal 240; CE Instruments Ltd., Italy). The weight of the sample used for the measurement was 0.7 g. Their microstructures were observed using a field emission scanning electron microscope (FE–SEM, S4500; Hitachi High-Technologies Corp., Tokyo, Japan).

3. Results and discussion

3.1. Single-step sintering

Fig. 2 shows the pore size distribution and cumulative volume of the green bodies before sintering. The average pore size was about 73 nm. It shows a sharp peak at the average

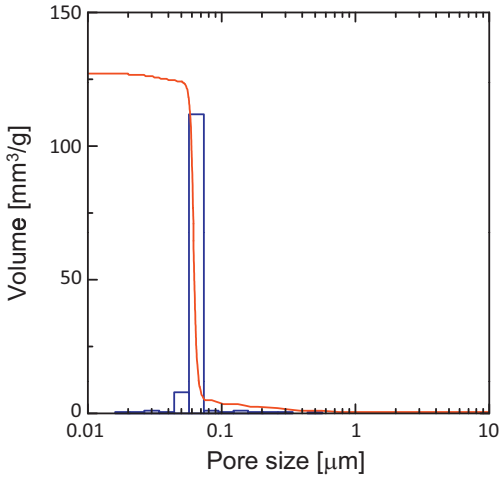

Fig. 2. Pore size distribution and cumulative volume of the sample before sintering.

value. The microstructure of the present sample is also depicted in Fig. 3. The α-Al_2O_3 particles were packed randomly. No large pore or cracking was observed. The porosity measured using Archimedes' technique was about 42%. Fig. 4 and Table 2 presents the average pore size and porosity as a function of sintering temperature. The pores of all samples were mainly open pores. With heating at less than 1000 °C, the porosities and the average pore size were mostly constant. With heating at temperatures greater than 1100 °C, the average pore size decreased with the increasing of the sintering temperature. The sample sintered at 1250 °C has 22 nm average pore size. The pore size distribution of the samples sintered at temperatures higher than 1300 °C could not be measured because the samples have low porosity. The porosity change was observed at a slightly lower temperature. Porosity reached 2% at more than 1300 °C. It is considered that these changes cause shrinkage during sintering.

The linear shrinkage rate of the samples was estimated. Fig. 5 shows the relation between the sintering temperature and linear shrinkage. The linear shrinkage of the samples was not changed significantly after heating below 1100 °C. However, it was increased significantly after heating to 1100 °C or higher temperatures. This behavior showed agreement with that described in previous reports [28]. The validity of these results was confirmed using calculations. The linear shrinkage, β, was

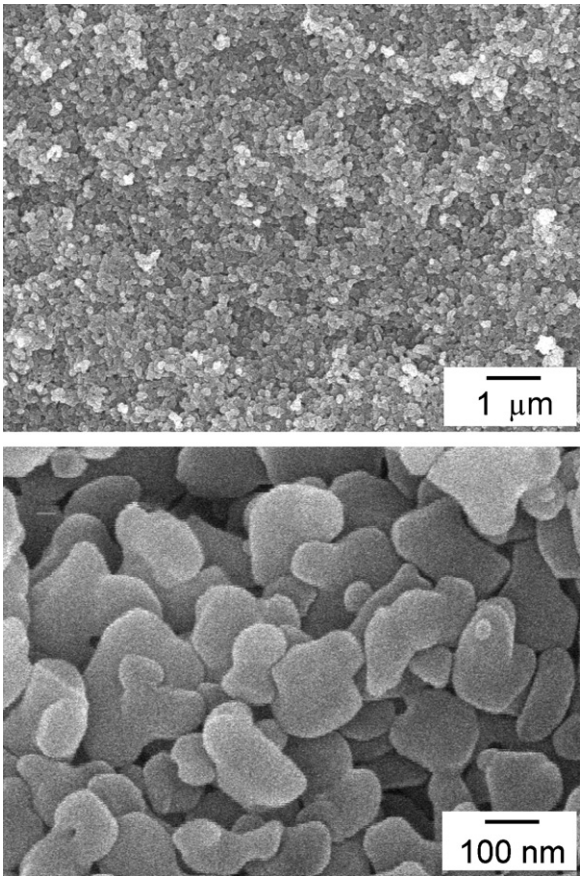

Fig. 3. FE-SEM micrographs of the samples before sintering.

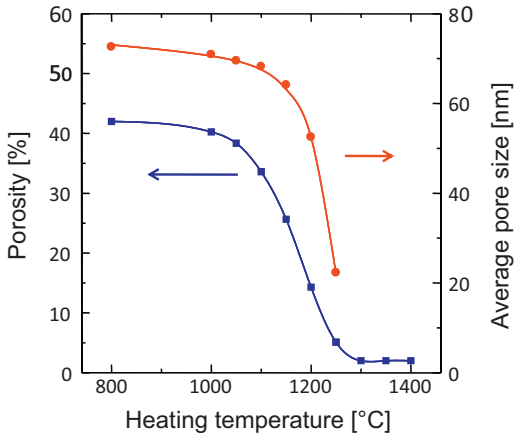

Fig. 4. Porosity and average pore size of the samples sintered using the single-step sintering method.

predicted using the following equation.

$$\beta = \frac{\sqrt[3]{1/\rho_1} - \sqrt[3]{1/\rho_2}}{\sqrt[3]{1/\rho_1}} \quad (2)$$

Therein, ρ_1 and ρ_2, respectively denote the relative density of the green body and the samples heated at various temperatures. The curve calculated using Eq. (2) is shown as a dotted line in Fig. 5. This curve fits well with the measured value, which indicates that no severe defects and orientation of the Al_2O_3 particles were present in the samples.

3.2. Optimum T_2 for two-step sintering

Fig. 6 shows the average pore size and porosity of the samples sintered using the program A. The average pore size and porosity of the sample sintered at 1100 °C as T_1 were, respectively, 74 nm and 36%. The pore size of the sample sintered at 1150 °C as T_1 is about equal to the value shown above. However, it decreased concomitantly with increasing T_1.

When the ceramics are prepared using two-step sintering method, T_1 is the temperature at which the grain boundary migration is active. Actually, T_2 should be set to a temperature at which the diffusion of atoms is sufficiently active without movement of the particles. These temperatures can be inferred

Table 2
Porosity and average pore size of the a-Al_2O_3 ceramics prepared using single-step sintering.

Sintering temperature (°C)	Porosity (%)	Average pore size (nm)
800	42	73
1000	40	71
1050	38	70
1100	34	68
1150	26	64
1200	14	53
1250	5	22
1300	<2	–
1350	<2	–
1400	<2	–

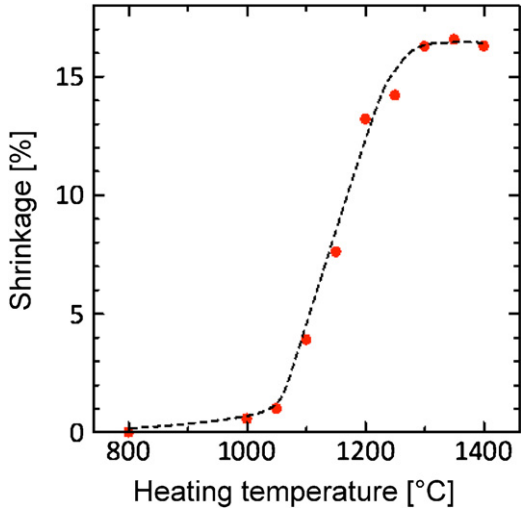

Fig. 5. Measured shrinkages of the samples sintered using single-step sintering method and shrinkage calculated using Eq. (2).

from the shrinkage curve of the sample sintered using one-step sintering. In Fig. 5, the samples shrank gradually at temperatures lower than 1050 °C and changed dynamically at 1050 °C and higher temperatures, which indicated that grain boundary migration was active at 1050 °C and higher temperatures. Therefore, when T_1 and T_2 were higher than the temperature of 1050 °C, both the pore size and porosity decreased, as they did in the general two-step sintering method. To obtain the results described in Section 3.3, T_2 was set as 1000 °C.

The sample microstructures were also verified. The FE–SEM micrographs of the samples sintered at 1000 °C as T_2 are portrayed in Fig. 7(a). The Al_2O_3 particle shape and size did not change much from those observed before sintering. At 1100 °C as T_2, some particles were round. The particles that mutually adhered are portrayed in Fig. 7(c). Sintering of the powder compacts was promoted at 1200 °C as T_2; grain growth was observed (Fig. 7(d)). It is inferred that this microstructural change well explained the results, as depicted in Fig. 6.

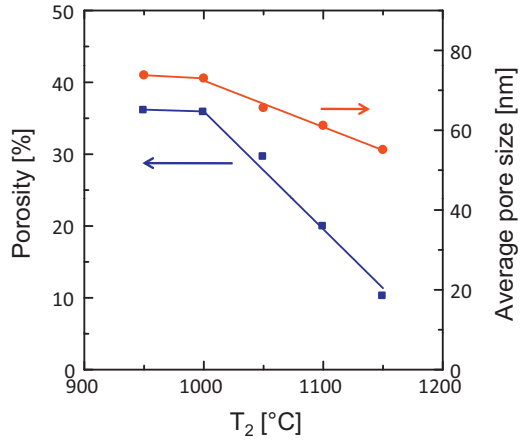

Fig. 6. Porosity and average pore size of the samples sintered using two-step program A.

3.3. Optimum T_1 for two-step sintering

The samples prepared using program B are presented in Fig. 8. The respective porosity and the average pore size of the samples sintered at 1050 and 1100 °C as T_1 were about 42% and 73 nm, which were the same as those of the samples before sintering. They also decreased concomitantly with increasing T_1 at 1150 °C and higher temperatures.

Porosity and the average pore size changes are considered to cause sintering shrinkage. This behavior resembles that of samples sintered using program A. However, the behaviors did not accord completely. Decreases of the pore size and porosity are regarded as originating in T_1. The sintering shrinkage showed slightly different behavior because the samples were cooled promptly after having arrived at T_1. The microstructures of the present samples are presented in Fig. 9. Data for 1150 °C as T_1 are displayed in Fig. 7(a). Particle adhesion was confirmed in both micrographs. However, the particles of these samples did not grow larger than the particles of the samples prepared using program A. This microstructural difference supports discussion of the slight difference between Figs. 6 and 8.

In the two-step sintering method, excessive energy is given to the particles at T_1 and is used for the diffusion of atoms at T_2 instead of that originally used for the grain boundary migration at T_1. The porosity and pore size of the samples after sintering at 1050 and 1100 °C as T_1 corresponded with the green body, which suggests that both temperatures are not sufficient to cause the diffusion of atoms. It also indicates that the promotion of the diffusion of atoms using one-step sintering is difficult. In contrast, samples sintered at 1150 °C as T_1 have a somewhat low value of the porosity. This temperature is expected to be ample for leading the initial driving force of the diffusion of atoms. Consequently, T_1 was selected as 1150 °C for this study.

3.4. Control of the pore size using two-step sintering

The green bodies were sintered at 1150 °C of T_1 and 1000 °C of T_2 for 2–12 h. The obtained data are presented in Fig. 10. The average pore size of the sample sintered for 2 h was about 61 nm. It increased concomitantly with increased sintering time, becoming about 73 nm after sintering for 12 h. However, the porosity was almost 35%.

In fact, T_1 of 1150 °C is the temperature at which the grain boundary migration and the diffusion of atoms with the movement of the particles are active. The porosity of the obtained samples decreased slightly from 42% to 35%. Furthermore, keeping temperatures at T_2 does not work for densification. This process is regarded as similar to the initial stage of sintering [29]. In this stage, the atomic diffusion is explained by the evaporation–condensation mechanism, surface and volume diffusion. The following equation shows the evaporation–condensation mechanism [29].

$$\frac{x}{r} = \left(\frac{3\sqrt{\pi}\gamma M^{3/2} p}{\sqrt{2}R^{3/2}T^{3/2}d^2}\right)^{1/3} r^{-2/3}t^{1/3} \quad (3)$$

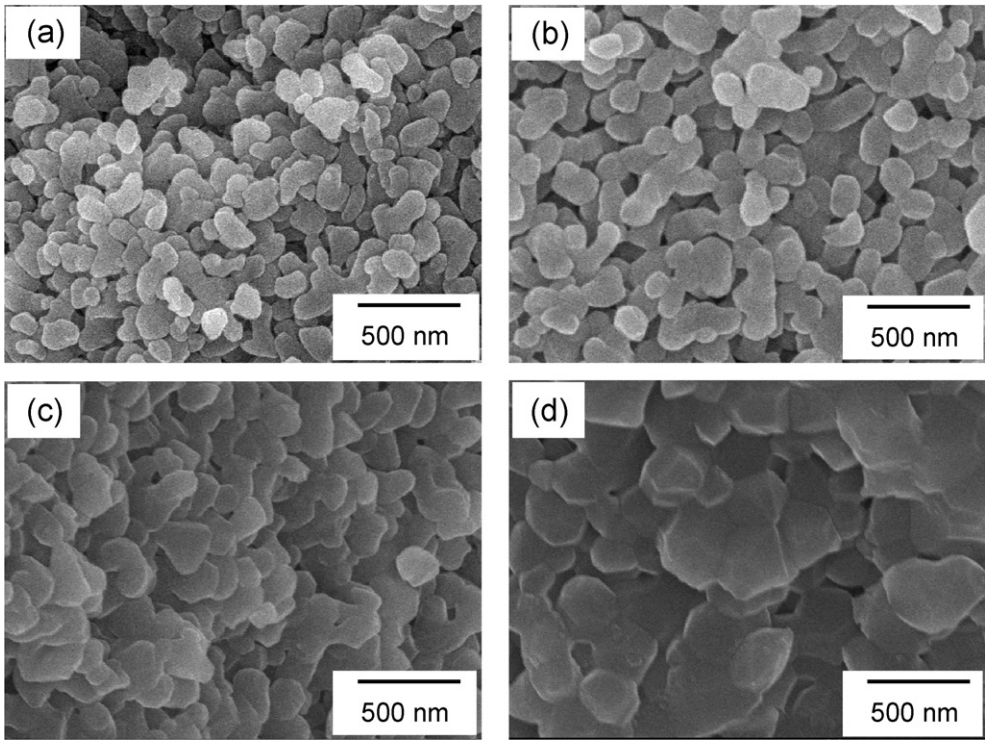

Fig. 7. FE-SEM micrograph of the samples sintered using two-step program A: T_2: (a) 1000 °C, (b) 1050 °C, (c) 1100 °C, and, (d) 1150 °C.

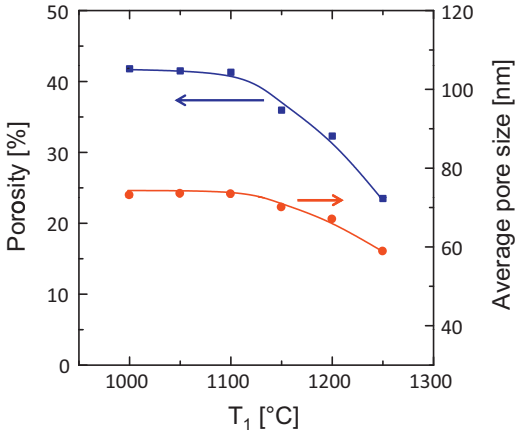

Fig. 8. Porosity and average pore size of the samples sintered using two-step program B.

Therein, x, r, γ, M, P, R, T, d, and t, respectively represent the neck size, particle radius, surface tension, molecular weight of the vapor, vapor pressure, ideal gas constant, absolute temperature, density, and sintering time. The equation shows that the long sintering time engenders neck growth and the decrease of the particle size. Furthermore, the distance between particles does not change because the atoms merely move from the surface of the neck. Similarly to the evaporation–condensation mechanism, the surface and volume diffusion do not decrease the porosity [29].

Based on these three sintering programs, we infer the following results. When T_1 and T_2 were set to temperatures higher than the temperature at which the grain boundary migration, the pore size and porosity decreased concomitantly with increased sintering temperature. When T_2 was set lower than this temperature, the pore size and porosity decreased concomitantly with increased sintering temperature. If T_1 is

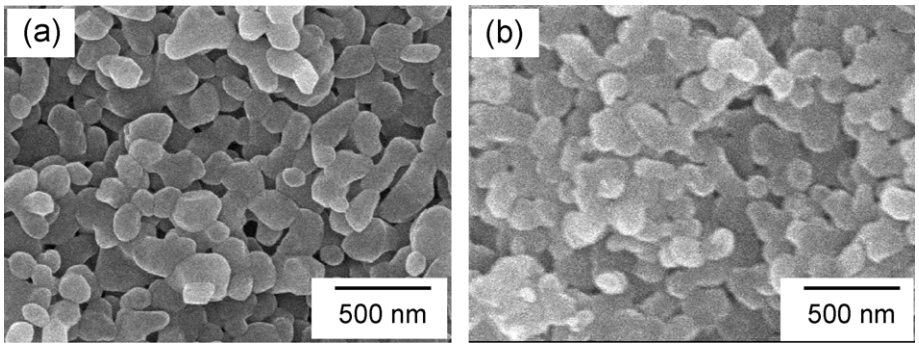

Fig. 9. FE-SEM micrograph of the samples sintered using two-step program B: T_1: (a) 1200 and (b) 1250 °C.

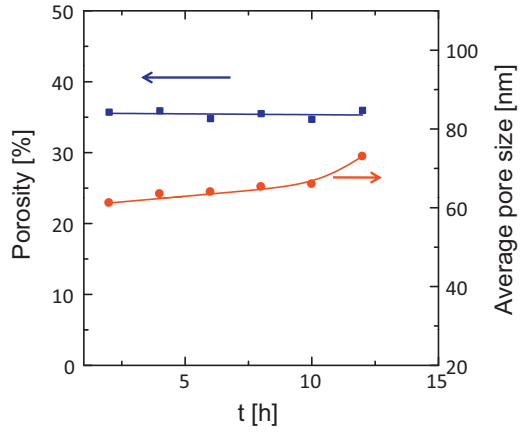

Fig. 10. Porosity and average pore size of the samples sintered using two-step program C.

insufficiently high, then neither the pore size nor porosity changed. When T_1 and T_2 are set higher and lower than the grain boundary migration, the pore size is controllable by the sintering time without porosity change.

4. Conclusions

Porous Al_2O_3 ceramics were prepared using a two-step sintering method. Porous ceramics having various pore size and porosity can be prepared precisely using the sintering program from the simple powder compact. The following results were obtained:

1. The porosities and the average pore size of the samples prepared using a one-step sintering method decreased concomitantly with increasing sintering temperature. The porosity was mostly constant at temperatures higher than 1300 °C. The porosity and average pore size curve as a function of the temperature shows typical sintering behavior.
2. For the two-step sintering method, the T_2 temperature is set to 1000 °C based on evaluation of the results of the samples prepared using program A. If the T_2 is higher than this temperature, then both porosity and pore size decease during sintering.
3. The T_1 temperature is set to 1150 °C from the results of the samples prepared by program B. When the T_1 temperature is lower than this temperature, the pore size and porosity do not change.
4. When T_1 and T_2 are set to 1150 and 1000 °C, which are the optimum temperatures, the pore size is controllable by the sintering time without porosity change. The average pore size of the obtained samples was 61–76 nm.

Acknowledgments

We are grateful to Professor E. Sakai of Tokyo Institute of Technology for permitting the use of mercury porosimetry. FE-SEM micrographs were taken at the Center for Advanced Materials Analysis (CAMA) of Tokyo Institute of Technology.

References

[1] A.R. Studart, U.T. Gonzenbach, E. Tervoort, L.J. Gauckler, Processing routes to macroporous ceramics: a review, J. Am. Ceram. Soc. 89 (2006) 1771–1789.
[2] J. Saggio-Woyansky, C.E. Scott, W.P. Minnear, Processing of porous ceramics, Am. Ceram. Soc. Bull. 71 (1992) 1674–1682.
[3] J. Luyten, I. Thijs, W. Vandermeulen, S. Mullens, B. Wallaeys, R. Mortelmans, Strong ceramic foams from polyurethane templates, Adv. Appl. Ceram. 104 (2005) 4–8.
[4] J.T. Richardson, Y. Peng, D. Remue, Properties of ceramic foam catalyst supports: pressure drop, Appl. Catal. A: General 204 (2000) 19–32.
[5] J. Luyten, S. Mullens, J. Cooymans, A.M. De Wilde, I. Thijs, New processing techniques of ceramic foams, Adv. Eng. Mater. 5 (2003) 715–718.
[6] T. Ota, M. Takahashi, T. Hibi, M. Ozawa, S. Suzuki, Y. Hikichi, H. Suzuki, Biomimetic process for producing SiC "Wood", J. Am. Ceram. Soc. 78 (1995) 3409–3411.
[7] T. Ota, M. Imaeda, H. Takase, M. Kobayashi, N. Kinoshita, T. Hirashita, H. Miyazaki, Y. Hikichi, Porous titania ceramic prepared by mimicking silicified wood, J. Am. Ceram. Soc. 83 (2000) 1521–1523.
[8] M. Mizutani, H. Takase, N. Adachi, T. Ota, K. Daimon, Y. Hikichi, Porous ceramics prepared by mimicking silicified wood, Sci. Technol. Adv. Mater. 6 (2005) 76–83.
[9] P. Colombo, E. Bernardo, L. Biasetto, Novel microcellular ceramics from a silicone resin, J. Am. Ceram. Soc. 87 (2004) 152–154.
[10] I. Thijs, J. Luyten, S. Mullens, Producing ceramic foams with hollow spheres, J. Am. Ceram. Soc. 87 (2004) 170–172.
[11] D.M. Liu, Densification and anisotropic shrinkage of die-pressed SiC of different granular forms, Ceram. Int. 23 (1997) 135–139.
[12] T. Isobe, Y. Kameshima, A. Nakajima, K. Okada, Y. Hotta, Gas permeability of the porous alumina ceramics with unidirectionally aligned pores, J. Eur. Ceram. Soc. 27 (2007) 53–59.
[13] T. Isobe, Y. Kameshima, A. Nakajima, K. Okada, Y. Hotta, Extrusion method using nylon 66 fibers for the preparation of porous alumina ceramics with oriented pores, J. Eur. Ceram. Soc. 26 (2006) 2213–2217.
[14] T. Isobe, T. Tomita, Y. Kameshima, A. Nakajima, K. Okada, Preparation and properties of porous alumina ceramics with oriented cylindrical pores produced by an extrusion method, J. Eur. Ceram. Soc. 26 (2006) 957–960.
[15] J. Zeschky, T. Hofner, C. Arnold, R. Weissmann, D. Bahloul-Hourlier, M. Scheffler, P. Greil, Polysilsesquioxane derived ceramic foams with gradient porosity, Acta Mater. 53 (2005) 927–937.
[16] E.J.A.E. Williams, J.R.G. Evans, Expanded ceramic foam, J. Mater. Sci. 31 (1996) 559–563.
[17] T. Tomita, S. Kawasaki, K. Okada, A novel preparation method for foamed silica ceramics by sol–gel reaction and mechanical foaming, J. Porous Mater. 11 (2004) 107–115.
[18] P. Sepulveda, J.G.P. Binner, S.O. Rogero, O.Z. Higa, J.C. Bressiani, Production of porous hydroxyapatite by the gel-casting of foams and cytotoxic evaluation, J. Biomed. Mater. Res. 50 (2000) 27–34.
[19] F.S. Ortega, J.A. Rodrigues, V.C. Pandolfelli, Strength of gelcast ceramic foams, Am. Ceram. Soc. Bull. 83 (2004) 9501–9506.
[20] R.L. Coble, Initial sintering of alumina and hematite, J. Am. Ceram. Soc. 41 (1958) 55–62.
[21] S.J. Glass, D.J. Green, Permeability and infiltration of partially sintered ceramics, J. Am. Ceram. Soc. 82 (1999) 2745–2752.
[22] S.Y. Shan, J.F. Yang, J.Q. Gao, W.H. Zhang, Z.H. Jin, R. Janssen, T. Ohji, Porous silicon nitride ceramics prepared by reduction–nitridation of silica, J. Am. Ceram. Soc. 88 (2005) 2594–2596.
[23] I.H. Arita, V.M. Castano, D.S. Wilkinson, Synthesis and processing of hydroxyapatite ceramic tapes with controlled porosity, J. Mater. Sci.: Mater. Med. 6 (1995) 19–23.
[24] D. Hardly, D.J. Green, Mechanical properties of a partially sintered alumina, J. Eur. Ceram. Soc. 15 (1995) 769–775;
I.-W. Chen, X.-H. Wang, Sintering dense nanocrystalline ceramics without final-stage grain growth, Nature 404 (2000) 168–171.

[25] K. Maca, V. Pouchly, P. Zalud, Two-step sintering of oxide ceramics with various crystal structures, J. Eur. Ceram. Soc. 30 (2010) 583–589.
[26] Z. Razavi Hesabi, M. Haghighatzadeh, M. Mazaheri, D. Galusek, S.K. Sadrnezhaad, Suppression of grain growth in sub-micrometer alumina via two-step sintering method, J. Eur. Ceram. Soc. 29 (2009) 1371–1377.
[27] T. Isobe, A. Ooyama, Y. Kameshima, A. Nakajima, K. Okada, Instrument for ceramic particle dispersion, Powder Technol. 200 (2010) 25–29.
[28] T. Isobe, Y. Hotta, Y. Kinemuchi, K. Watari, Preparation and mechanical properties of the Al_2O_3 ceramics from wet-jet milled slurry, J. Ceram. Soc. Jpn. 115 (2007) 738–741.
[29] W.D. Kingery, Introduction to Ceramics, Wiley, New York, 1960.